



STRUCTURAL AND THERMAL INVESTIGATIONS OF ROLLING TIRES IN A FLAT ROAD

Thanh Cong Nguyen^{1*}, Khanh Duy Do Cong², Cong Truong Dinh²

¹University of Transport and Communications, No 3 Cau Giay Street, Lang Thuong Ward, Dong Da District, Ha Noi 11512, Vietnam

²Hanoi University of Science and Technology, No 1, Dai Co Viet Road, Hai Ba Trung District, Hanoi 11615, Vietnam

ARTICLE INFO

TYPE: Research Article

Received: 10/08/2022

Revised: 18/10/2022

Accepted: 26/11/2022

Published online: 15/01/2023

<https://doi.org/10.47869/tcsj.74.1.5>

* *Corresponding author*

Email: congnt@utc.edu.vn

Abstract. Rubber is an essential component of a pneumatic tire. In general, the tire, or the rubber part, is heated by the hysteresis effects caused by the deformation of the rubber part during the operation. Besides, the tire temperature depends on many factors, such as inflation pressure, vehicle loading, car speed, road tire, environment condition, and tire geometry, etc. This study focuses on the finite element approach to compute by simulating the temperature distributions of a steady-state rolling tire. For simplicity, the tire is assumed to be composed of rubber, body-ply, wire, and rim only. The nonlinear mechanical behavior of the rubber is characterized by a Mooney–Rivlin model, while the other parts are assumed to be a linear elastic material. The coupled effects of the inflation pressure and vehicle loading are investigated. Hysteresis energy loss is used as a bridge to link the strain energy density to the heat source in rolling tires. The steady-state thermal analysis may obtain the temperature distribution of rolling tires. On the other hand, an efficient computational process is being introduced to decrease the time for coupled 3D dynamic rolling simulation of the tire. The simulation results show that loading is the main factor in determining the temperature field.

Keywords: Tire structure, thermal investigation, rolling tires, friction heat, ANSYS ICEM.

1. INTRODUCTION

Tire temperature is one of the leading causes of tire fatigue and affects tire integrality and effectiveness [1]. Temperature rise within a tire occurs for two reasons: Friction between treads and roads and internal heat generation due to the repeated deformation of the rubber material. Many experiments were investigated to evaluate the temperature rise within the rubber material in accordance with its composition [2, 3].

Many researchers have been predicting tire temperature through simulation. Park [4] indicated a numerical process to process the temperature distribution of a rolling tire during the steady-state simulation. During the process, the strain and speed of the tire were evaluated with a mechanical solver. Then, the energy dissipation rate of the viscoelastic rubber was assessed. Lastly, the temperature distribution of the tire was derived using a thermal solver. Nevertheless, this approach has its negativity because it can only be adopted for steady-state analysis.

Johnson [5] and Kan et al. [6] performed a thermo-mechanical coupled problem in cyclic loading analysis using Abaqus. They concluded that the stress and thermal analyses are valid for large strains and displacements. Luo [7] solved a coupling problem based on a staggered approach by combining the Abaqus user subroutines of UMASFL, USDFLD, HETVAL, and UEXTERNALDB. Tang [8] also predicted the temperature distribution of a steady-state rolling tire. They decreased the high-temperature area and moved to the shoulder position as the inflation pressure increased. The finite element technique (FEM) was used in numerous studies to analyze tire stress and temperature [9].

However, these studies were induced with steady-state transport analysis. In which tire deformation due to contact with the road is calculated as one stage only. Moreover, the actual deformation of a rolling tire influenced by road conditions are not considered, and it even causes error in estimating temperature change. Nevertheless, examining the interior temperature change within a tire is relatively challenging because the tire and its rim are mounted using high-inflated pressure and the rolling phenomenon.

This study proposes a method for numerical simulation to predict internal temperature rise within a tire at different speeds, inflation pressure, and loading. Our methodology employs two significant sections. First, the structural analysis of a rolling tire in contact with the road is performed with transient analysis to evaluate the effect of the tire on the road correctly. The heat generation rate can be obtained from the hysteresis energy losses. Total strain energy was obtained by dynamic rolling simulation of the tire. Under hysteresis data derived from a dynamic mechanical analyzer, hysteresis energy losses could be derived and used to predict the temperature distribution by steady-state thermal analysis.

2. THEORETICAL MODELS OF RUBBER MATERIALS

2.1. Hyperelastic Mooney–Rivlin material model

Rubber is the main element of the tire. It can absorb vibration and deformation under different conditions. Cord plies are mounted in the rubber part and prevent overwhelming deformation for the rubber. The bead wire is the stiffening material in the tire to constrain the deformation of both rubber and cord ply. Tires deform repeatedly and rapidly during high-speed driving, and their viscoelastic behavior leads to hysteresis. The temperature of a tire rises from the heat generation due to the hysteresis effect, which is released from the deformation of the tire. An overall discussion of the material characteristics is given in Gehman's study [10].

2.2. Heat generation rate

In this study, strain energy density and hysteresis will be used to calculate the heat generated within a rolling tire. The total strain energy density that is calculated from the deformation module is multiplied by the hysteresis to find the lost strain energy density as:

$$U_{loss} = H \cdot U_{total} \quad (1)$$

The lost strain energy density is the energy that is not recovered after deformation, which is assumed to contribute to internal heat generation in this study completely. Frequency is defined as the velocity divided by the circumference of the rolling tire with the following equation:

$$f = \frac{v}{2\pi R} \quad (2)$$

Once the frequency of the rolling tire is found, it is multiplied by the lost strain energy density to calculate the heat generation rate per unit volume (W/m^3) for each element:

$$H_G = U_{loss} \cdot f \quad (3)$$

3. SIMULATION METHODOLOGY

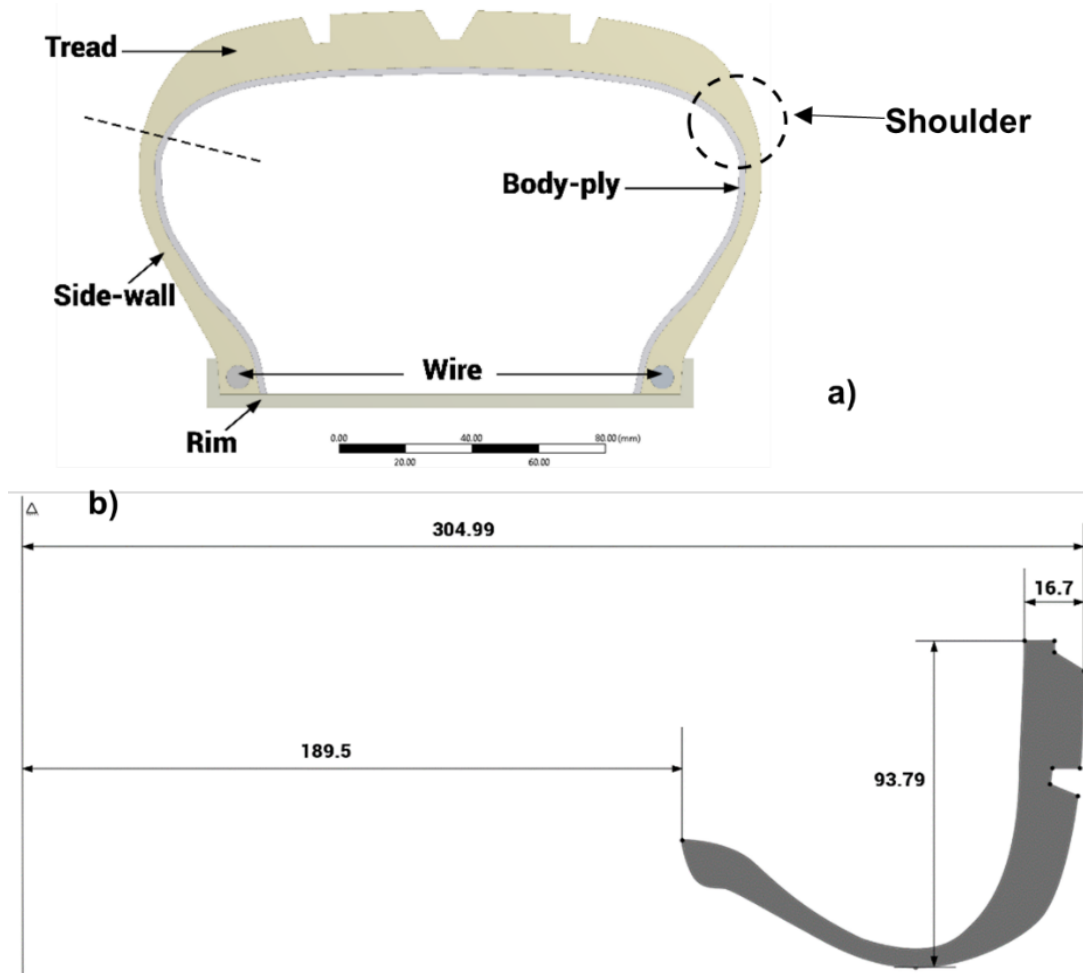


Figure 1. The axisymmetric cross-section of an inflated tire (185/60 R15): (a) tire components. (b) Tire size, unit (mm).

The size of a standard passenger tire (185/60 R15) was used for the simulations in this work. The size and cross-section of the rubber of the tire are shown in Fig. 1. To simplify the problem, some reasonable assumptions and simplifications were made for the simulations:

- Assume that the tire consists of rubber, cord plies, steel wires, and a rim.
- Rubber is assumed to be isotropic, homogeneous, and has hyper-elastic behavior through the entire temperature range.
- The cord ply, rim, and steel wire are elastic, isotropic, and homogeneous.
- The road is assumed to be rigid.
- Assume the friction coefficient between the road and tire is a constant: 0.1.

Material properties are summarized in Table 1. The mechanical and thermal properties of bead wire were taken as stainless steel.

Table 1. Material properties used in the simulation

Material	Rubber	Body-ply	Wire
Density (kg/m ³)	1400	1200	6500
Poisson's ratio	-	0.3	0.3
Young's modulus (MPa)	-	500	207x10 ⁹
Mooney-Rivlin constant (MPa)	C ₁₀ =8.061 C ₀₁ =1.805	-	-
Thermal conductivity (W/m.°C)	0.293	0.293	60.5
Hysteresis	0.1	-	-

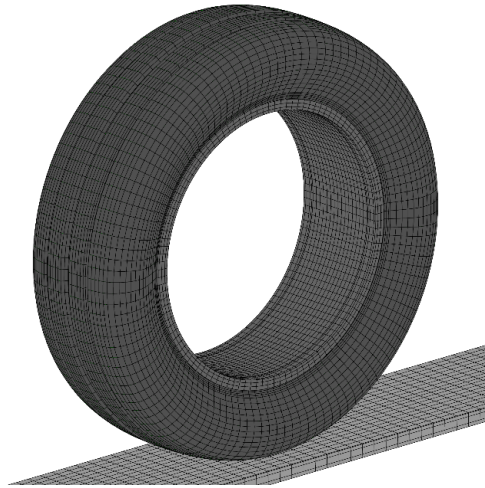


Figure 2. Mesh for the simulation.

The mesh for the simulation is constructed using structural mesh using ANSYS ICEM. The overall simulation mesh is shown in Fig. 2. The software package employed for simulation work was provided by ANSYS, Inc, which includes ANSYS Transient Mechanical and ANSYS Steady-state thermal version 19.1.

3.1. Dynamic rolling analysis

As the transient behavior of a rolling tire is in a transient state, it would elongate the computational time cost to obtain the steady-state solution. Hence, an effective procedure was introduced to simulate the rolling conditions. The dynamic rolling analysis was separated into

two stages:

a. Step 1: Loading analysis

The tire is simulated under different pressures and loadings with static-state mechanical simulations. The displacements are then obtained under a non-rotating state [11]. Different loadings (1, 2, 3, 4, 5, 6kN) were applied to the rim, and an inflation pressure of 30 psi was applied at the inner surfaces of the tire. The boundary conditions for loading analysis are demonstrated in Fig. 3.

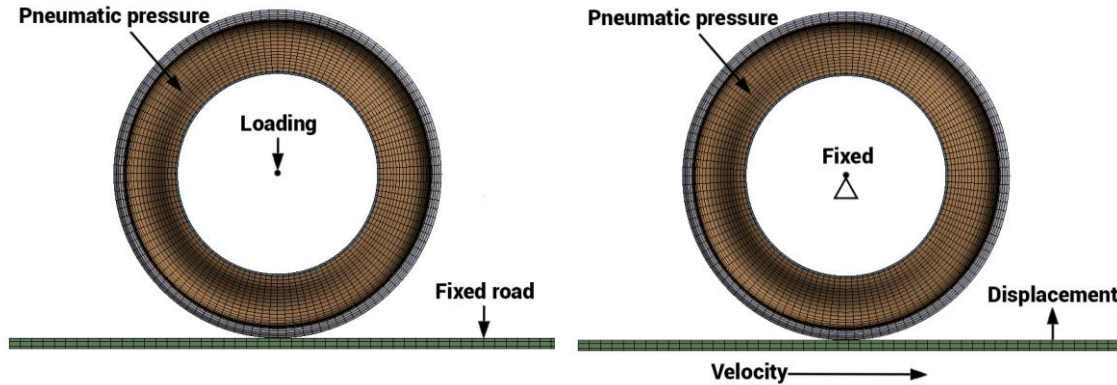


Figure 3. Boundary conditions for loading analysis Figure 4. Boundary conditions for rolling analysis.

b. Step 2: Rolling analysis

The displacement results from step 1 were set as the boundary conditions for the upward displacement of the road. Different velocities were applied to the road component to simulate the rolling effect, and the rim is assumed with a fixed displacement of any direction but free rolling. After the study, the total strain energy density of the tire is obtained. This step is performed in transient analysis, so that it would take more time than step 1. The boundary conditions applied in the rolling study are shown in Fig. 4.

3.2. Steady-state thermal analysis

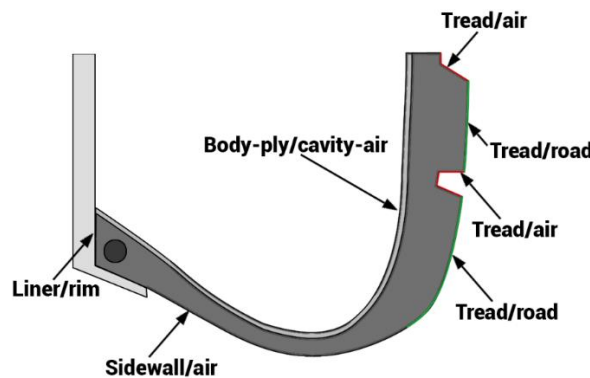


Figure 5. Thermal boundary conditions for heat transfer analysis of tire.

Table 2. Heat transfer coefficients used for thermal boundary conditions in thermal module.

Boundary condition location	Heat transfer coefficient (W/m ² .°C)	Sink temperature (°C)
Tread/road	12000	25
Tread/air	16.18	25
Sidewall/air	16.18	25

Body-ply/cavity-air	5.9	38
Liner/rim	88000	25

The heat generation rate (H_G) was applied for all rubber elements as the primary heat source. The mesh of the thermal analysis is identical to the 3D mesh of the structural analysis. The heat transfer coefficients are taken from the literature [4] and summarized in Table 2. The sink temperatures are assumed to be 25 °C for the ambient air, all tire components, and the road surface. The temperature of the air inside the tire is set as 38 °C. Fig. 5 demonstrates the different boundary conditions on different surfaces.

4. SIMULATION RESULTS AND DISCUSSIONS

4.1. Loading analysis

In this subsection, the loading analysis is carried out with varying loading from 1 to 6kN by the step of 1kN. The inflated pressure is kept at 30psi. The displacements are then recorded and compared with the data from the report of Lin and Hwang [12]. The results are shown in Fig. 6.

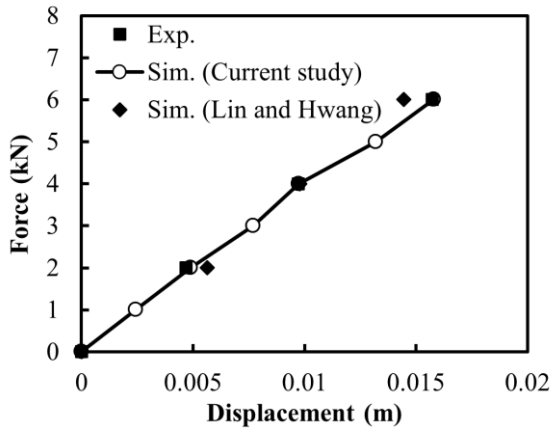


Figure 6. Comparison of numerical and experimental results.

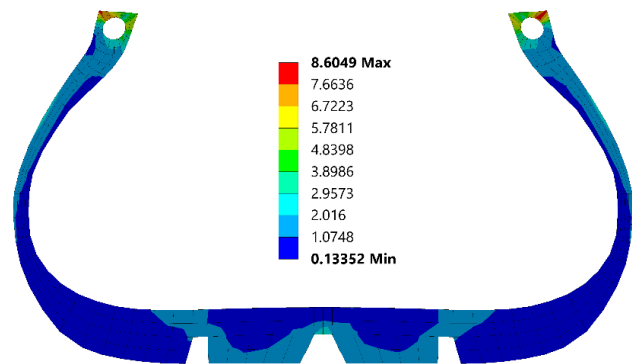


Figure 7. Distribution of equivalent von-Mises stress on the rubber (Unit: MPa).

The visualization shows that the results from the present study are in better agreement with both the experimental data than the results from Lin and Hwang [12] themselves. The maximum deviation of all cases with the experimental data is roughly 4%. Hence, the reliability of the numerical method has been rationally authenticated.

4.2. Rolling analysis

The contour plots of von-Mises stress on the rubber part of a steady-state rolling tire at inflated pressure of 32psi, loading of 3kN, and $V = 80$ km/h is shown in Fig. 7. It can be observed that the regions near the stiffer part are the principal load-carrying elements. Thus, the magnitude of stress undertaken by rubber is significantly reduced.

4.3. Thermal analysis

In this subsection, the process of investigating thermal distributions in the tire with different boundary conditions, i.e., inflated pressure, loading, and velocity, is demonstrated. The detailed ranges for the parametric study are shown in Table 3.

Table 3. Ranges for parametric study.

Parameters	Ref. Value	Min	Max	Step
Weight (kg)	300	100	600	100
Pressure (psi)	32	27	35	1
Velocity (km/h)	80	20	80	20

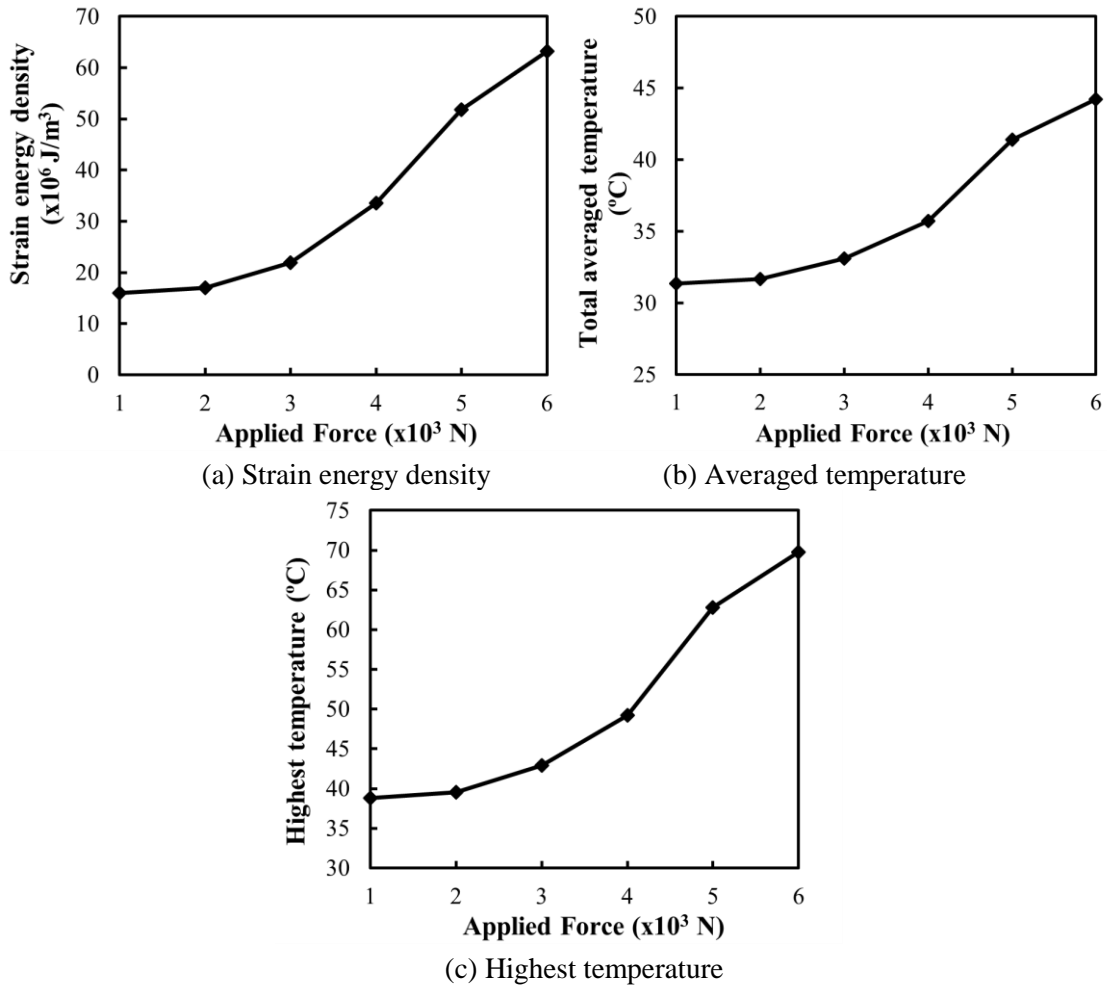


Figure 8. Variation of three variables with applied force.

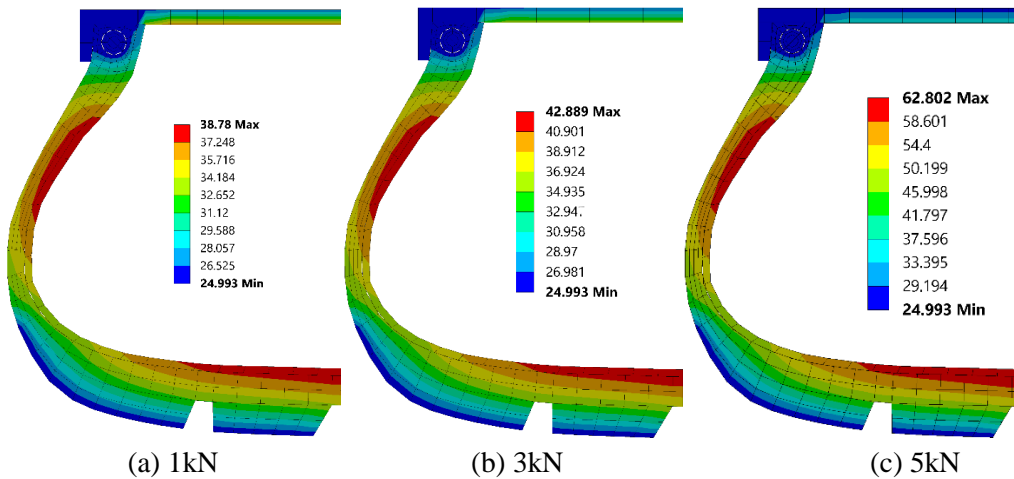


Figure 9. Distribution of temperature within rubber and body-ply with different loadings (unit: °C).

a. Change Loading

The variation of strain energy density averaged temperature, and highest temperature on all bodies are shown in Figs. 8(a), 8(b), and 8(c), respectively. It is found that all three variables increase when increasing the applied force. The maximum temperature on the tire is about 70°C at F=6kN. The distributions of temperature in a 2D cut section of half the tire are shown in Figs. 9(a), 9(b), and 9(c). It can be seen that the highest temperature areas are located in the shoulder and sidewall regions. These are the regions of highest deformation of the tire. Moreover, the bottom parts of the tire that are in contact with the air are also the regions with high temperatures because of the high deformation. The bottom parts in contact with the road should be at the highest temperature if the siping doesn't exist. However, the areas of high temperature slightly decrease in size when the loading increases.

b. Change pressure

The variation of strain energy density averaged temperature and total temperature with increasing inflated pressure are demonstrated in Figs. 10(a), 10(b), and 10(c). At first, when increasing the pressure from 27 to 29 psi, all three variables decrease, but the variables increase again when the pressure is increased from 29 to 35 psi. The variations of all three variables are lower than the increased rate of changing loading. The maximum temperature range is from 42.3 to 43.2 °C.

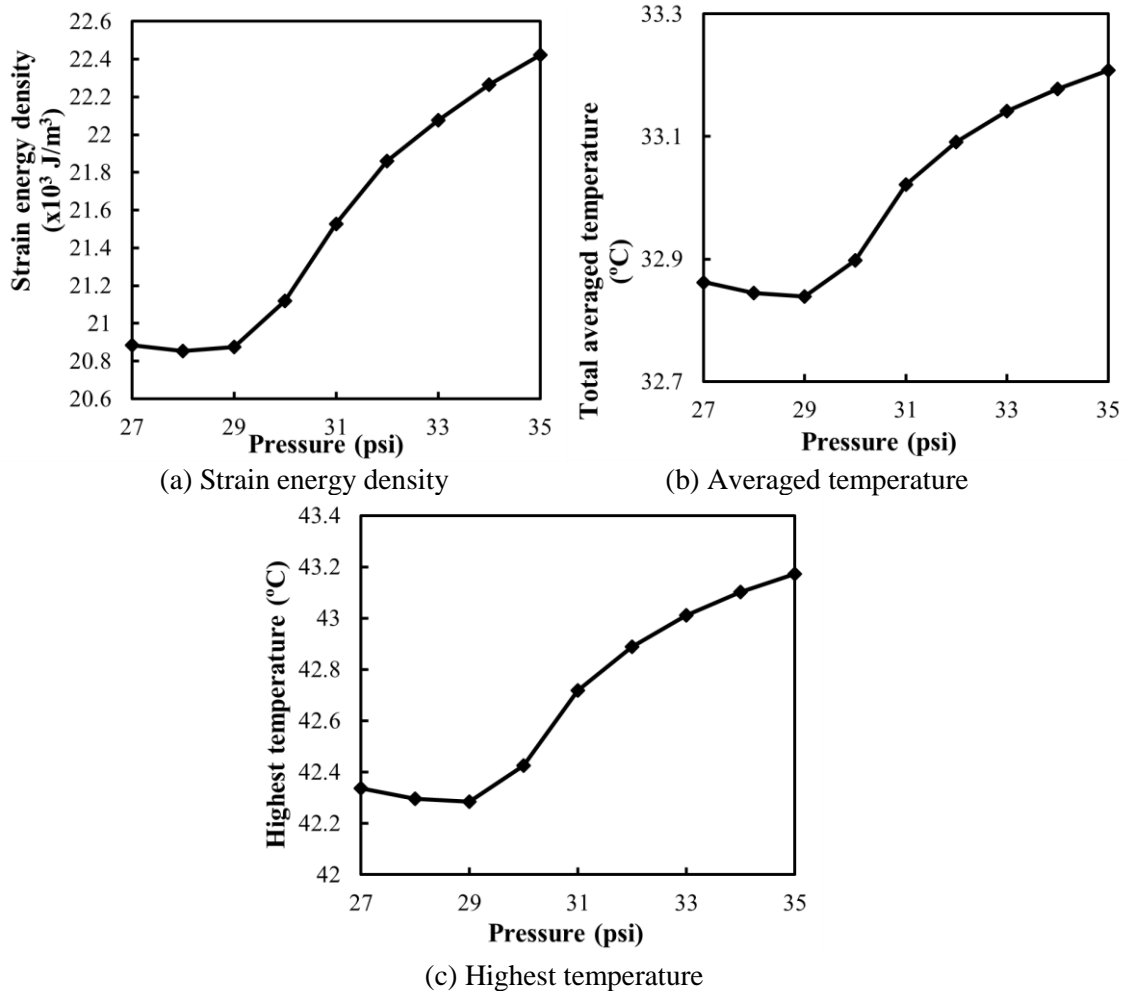


Figure 10. Variation of three variables with varying inflated pressure.

Figs. 11(a), 11(b), and 11(c) show the distributions of temperature on the 2D plane section of half the tire with the inflation pressure of 30, 32, and 34 psi. It is discovered that the regions of high temperature are at the same position as analyzed above. As the inflation pressure was increased, the high-temperature areas were slightly expanded.

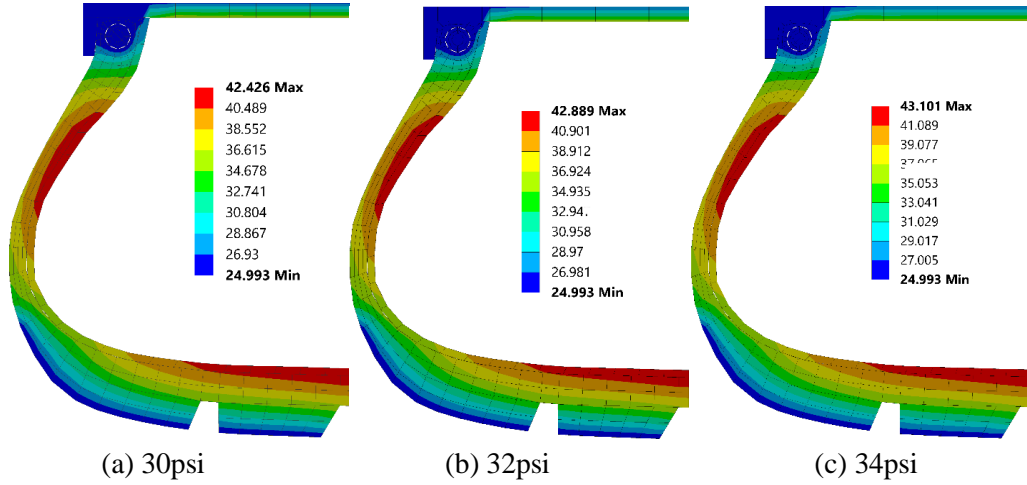


Figure 11. Distribution of temperature in rubber and body-ply with different pressure (unit: °C).

c. Change velocity

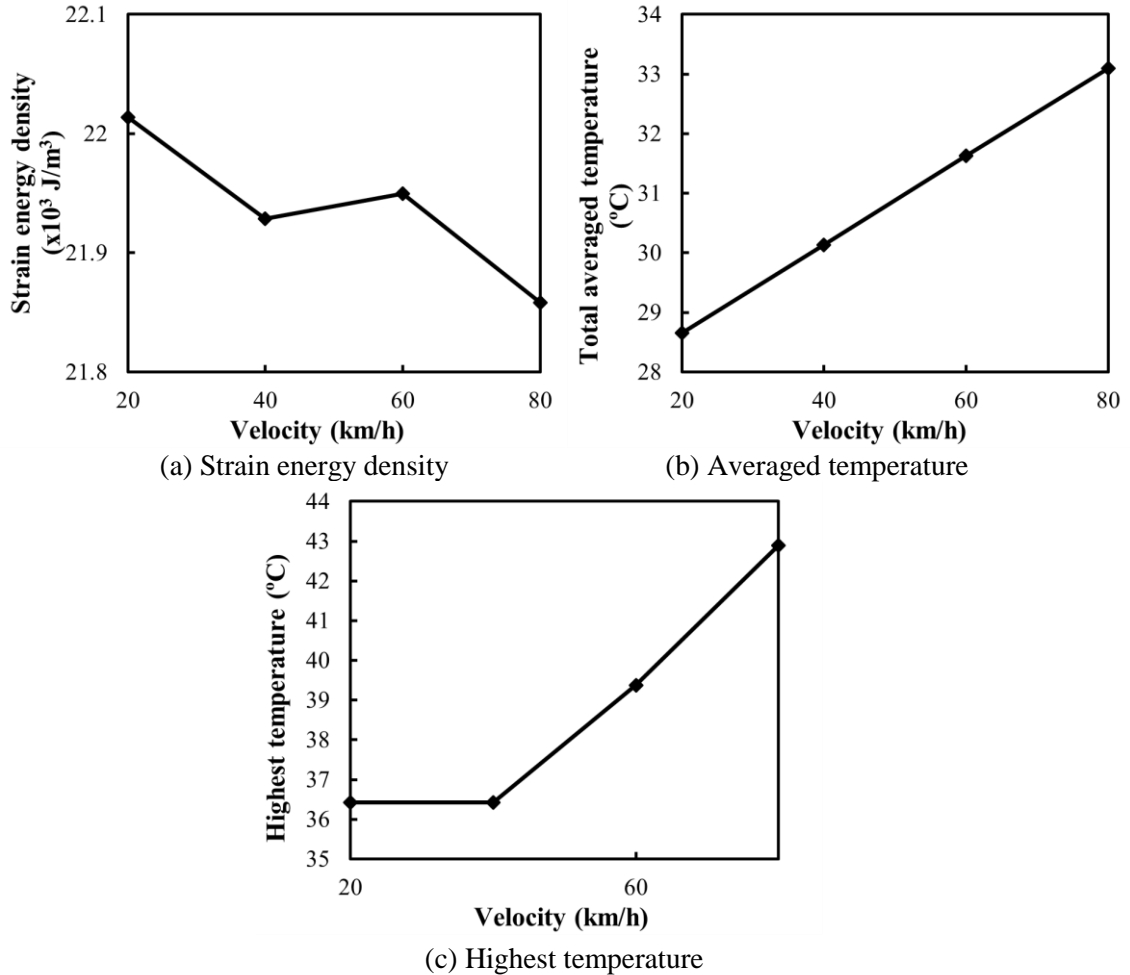


Figure 12. Variation of three variables with different velocity.

The development of strain energy density averaged temperature and highest temperature with changing speed are shown in Figs. 12(a), 12(b), and 12(c), respectively. Firstly, with changing velocity, the strain energy density is decreased from 20 to 40km/h. After that, it increases slightly from 40 to 60km/h and dramatically drops from 60 to 80km/h. Besides, the averaged temperature increases linearly with increasing speed. However, the total temperature of velocity 20 and 40 km/h is the same. It is due to the highest temperature regions of these two cases being located in the rim.

When considering the temperature distribution on the cross-section of half the tire in Figs. 13(a), 13(b), and 13(c). It is also found that the temperature at the inner surface is higher than at the outer surface because of the convection through the air at the inner surface. Moreover, the maximum temperature of the tire rises along with the expansion of the high-temperature regions when increasing the velocity. With the speed of 80km/h, the highest temperature on the tire is much higher than that on the rim.

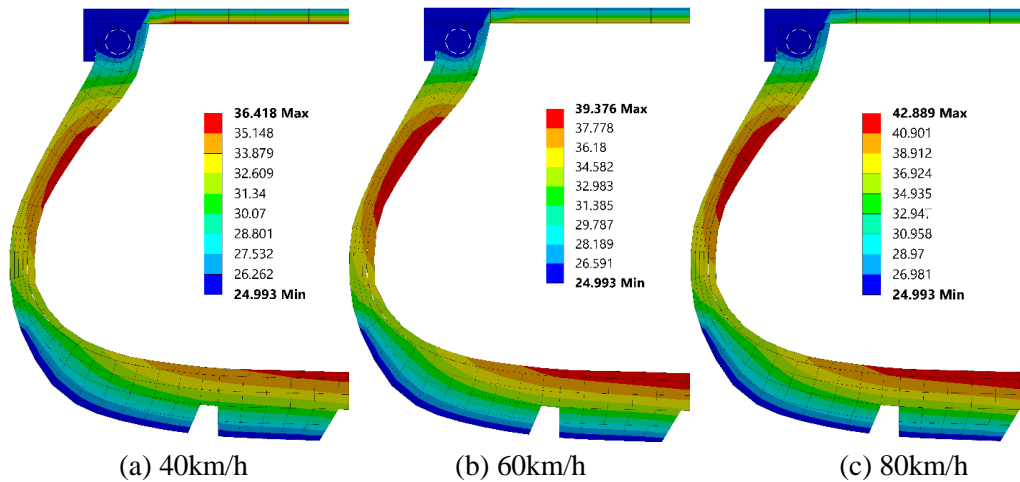


Figure 13. Distribution of temperature in rubber and body-ply with different velocities (unit: °C).

Overall, increasing loading, pressure, or speed increases the temperature of the tire. Moreover, the increase in loading has a more severe effect on the rise in tire temperature than the increase in inflated pressure and velocity.

5. CONCLUSION

The temperature rise in the tire during normal operating conditions is investigated in this work. Besides, a parametric study of boundary conditions is carried out to study the effect of changing conditions on the varying temperature distribution inside the tire. The mesh is composed of hexahedral elements. The results are then compared with experimental data. The results show that the effect of loading on the temperature of the tire is more severe than the inflated pressure and velocity. The maximum temperature is achieved as 70°C at a pressure of 32psi, a velocity of 80km/h, and a loading of 6kN. Moreover, the maximum temperature is increased with the rise of all three variables. However, the regions of high-temperature decrease when the three variables are enlarged.

The future work will focus on the effects of the road and rubber siping on the temperature distribution of the rubber part.

ACKNOWLEDGMENT

This research is funded by University of Transport and Communications (UTC) under grant number T2021-CK-003TĐ.

REFERENCES

- [1]. T. G. Ebbott, R. L. Hohman, J. P. Jeusette, V. Kerchman, Tire temperature and rolling resistance prediction with finite element analysis, *Tire Science & Technology*, 27 (1999) 2-21. <https://doi.org/10.2346/1.2135974>
- [2]. K. K. Kar, A. K. Bhowmick, Hysteresis loss in filled rubber vulcanizates and its relationship with heat generation, *Journal of Applied Polymer Science*, 64 (1997) 1541-1555. [https://doi.org/10.1002/\(SICI\)1097-4628\(19970523\)64:8<1541::AID-APP12>3.0.CO;2-0](https://doi.org/10.1002/(SICI)1097-4628(19970523)64:8<1541::AID-APP12>3.0.CO;2-0)
- [3]. D. M. Park, W. H. Hong, S. G. Kim, H. J. Kim, Heat generation of filled rubber vulcanizates and its relationship with vulcanizate network structures, *European Polymer Journal*, 36 (2000) 2429-2436. [https://doi.org/10.1016/S0014-3057\(00\)00020-3](https://doi.org/10.1016/S0014-3057(00)00020-3)
- [4]. H. C. Park, S. K. Youn, T. S. Song, N. J. Kim, Analysis of temperature distribution in a rolling tire due to strain energy dissipation, *Tire Science & Technology*, 25 (1997) 214-228. <https://doi.org/10.2346/1.2137541>
- [5]. A. R. Johnson, Coupled thermo-mechanical analysis of dynamically loaded rubber cylinders, Proc. of 32nd International SAMPE Technical Conference, Boston, USA (2000).
- [6]. Q. Kan, G. Kang, W. Yan, Y. Zhu, H. Jiang, A thermo mechanically coupled cyclic plasticity model at large deformations considering inelastic heat generation, Proc. of 13th International Conference on Fracture, Beijing, China (2013).
- [7]. R. K. Luo, X. P. Wu, A. Spinks, Heat generation analysis of a rubber wheel using the steady-state transport analysis capability in abaqus, Proc. of SIMULIA Customer Conference, London, England (2009).
- [8]. T. Tang, D. Johnson, E. Ledbury, T. Goddette, S. D. Felicelli, Simulation of thermal signature of tires and tracks, Proc. of Ndia Ground Vehicle Systems Engineering and Technology Symposium, Michigan, USA (2012).
- [9]. S. K. Clark (Ed.). *Mechanics of pneumatic tires*. US Government Printing Office (1981).
- [10]. Gehman, S. D. Material characteristics in mechanics of pneumatic tires, in: Clark S. K. (Ed.) (1981). *Mechanics of Pneumatic Tires*, Office of Vehicle Systems Research, Institute for Applied Technology and National Bureau of Standards, US Department of Commerce, Washington, pp. 1-40.
- [11]. Truong Manh Hung, Nguyen Thanh Cong, Research on the application of Ansys software to determining Automobile tire durability in Vietnam, *Transport and Communications Science Journal*, 3 (2021), 242-250. <https://doi.org/10.47869/tcsj.72.3.1>
- [12]. Y. J. Lin, S. J. Hwang, Temperature prediction of rolling tires by computer simulation, *Mathematics and Computers in Simulation*, 67 (2004) 235-249. <https://doi.org/10.1016/j.matcom.2004.07.002>